Nuclear structure of lowest ^{229}Th states and time-dependent fundamental constants

Elena Litvinova[1,2,3] and Hans Feldmeier[1]
[1]GSI Helmholtzzentrum für Schwerionenforschung, Planckstr. 1, D-64291 Darmstadt, Germany
[2]Frankfurt Institute for Advanced Studies, Ruth-Moufang-Str. 1, D-60438 Frankfurt am Main, Germany
[3]Institute of Physics and Power Engineering, RU-249033 Obninsk, Russia

Jacek Dobaczewski
Institute of Theoretical Physics, University of Warsaw, Hoża 69, PL-00-681 Warsaw, Poland and
Department of Physics, P. O. Box 35 (YFL), FI-40014 University of Jyväskylä, Finland

Victor Flambaum
School of Physics, University of New South Wales, Sydney, New South Wales 2052, Australia
(Received 18 December 2008; revised manuscript received 11 May 2009; published 2 June 2009)

The electromagnetic transition between the almost degenerate $5/2^+$ and $3/2^+$ states in ^{229}Th is deemed to be very sensitive to potential changes in the fine structure constant α. State of the art Hartree-Fock and Hartree-Fock-Bogoliubov calculations are performed to compute the difference in Coulomb energies of the two states that determines the sensitivity of the transition frequency ν on variations in α. The kinetic energies are also calculated that reflect a possible variation in the nucleon or quark masses. As the two states differ mainly in the orbit occupied by the last unpaired neutron the Coulomb energy difference results from a change in the nuclear polarization of the proton distribution. This effect turns out to be rather small and to depend on the nuclear model. The sensitivity q_s of the frequency shift $\delta\nu$ on $\delta\alpha/\alpha(\delta\nu = q_s\delta\alpha/\alpha)$ varies for the different models between about $+10^{20}$ Hz and -10^{20} Hz. Therefore, much more effort must be put into the improvement of the nuclear models before one can draw conclusions from a measured drift in the transition frequency on the size of a temporal drift of α.

DOI: 10.1103/PhysRevC.79.064303 PACS number(s): 21.60.Jz, 06.20.Jr, 27.90.+b

I. INTRODUCTION

Measurements of a suspected temporal variation of the fine structure constant α by means of atomic transitions have reached a limit for $\delta\alpha/\alpha$ of less than 10^{-16} per year [1–8]. A tempting idea to decrease the limit is to use the transition between two nuclear states with very different Coulomb energies, because the drift in transition frequency

$$\delta\nu = \frac{\Delta V_C}{h}\frac{\delta\alpha}{\alpha}, \tag{1}$$

according to the Hellmann-Feynman theorem, is given by the difference ΔV_C in Coulomb energies of the two states involved in the transition times the relative drift $\delta\alpha/\alpha$ [9]. The sensitivity $q_s = \Delta V_C/h$ on relative changes in α can be very large. Typical Coulomb energies in big nuclei are of the order of $V_C \approx 10^9$ eV so that even a small difference ΔV_C like 10^5 eV would give a sensitivity $q_s \approx 2 \times 10^{19}$ Hz.

A promising candidate for that is the transition between the $3/2^+$ isomeric state of the nucleus ^{229}Th to its $5/2^+$ ground state [10,11]. Recent measurements yield $h\nu = 7.6 \pm 0.5$ eV [12] that on nuclear energy scales is an accidental almost degeneracy. A sensitivity of 2×10^{19} Hz would transform a drift of 10^{-16} in $\delta\alpha/\alpha$ to a shift in frequency of $\delta\nu \approx 2000$ Hz. This implies that a measurement of $\delta\nu$ more accurate than 2000 Hz would improve the present limit on $\delta\alpha/\alpha$.

The accuracy for measuring $\delta\alpha/\alpha$ is in principle limited by the width Γ of the decaying state

$$\frac{\delta\alpha}{\alpha} = \frac{h\delta\nu}{\Delta V_C} \pm \frac{\Gamma}{\Delta V_C}. \tag{2}$$

Γ has been estimated in Refs. [13,14] to be of the order 10^{-17} to 10^{-19} eV corresponding to a lifetime $T_{1/2} = (50 \cdots 5000)$ s. Assuming again $\Delta V_C \approx 10^5$ eV reduces the uncertainty in $\delta\alpha/\alpha$ to 10^{-22} to 10^{-24}, see Eq. (2). This accuracy would be 6 to 8 orders of magnitude better than the presently reached 10^{-16} by atomic transitions.

The difference between a nuclear and an atomic transition is that in atomic transitions, both the frequency and the sensitivity are determined by the electromagnetic interaction and hence the sensitivity is always of the order of a few 10^{15} Hz [15–19]. In the nuclear case the transition frequency is mainly determined by the strong interaction and the sensitivity by the Coulomb energy. Therefore the nuclear energies contain a contribution linear in α, differing from the atomic case where the energies depend on α^2. For this reason the sensitivity q_s defined here differs from the atomic one by a factor of two.

A big drawback of this idea is that the Coulomb energies cannot be measured but have to be calculated with sufficient accuracy in a nuclear model. Differences in charge radii and quadrupole moments of the nuclear states are in principle experimentally accessible. Their measurement would reduce the uncertainty.

In a simplified picture the two states differ by the occupation of the last neutron orbit. The change in the Coulomb energy is thus due to a modified neutron distribution in the excited state that will polarize via the strong interaction the proton distribution in a slightly different way than in the ground state.

In this article we investigate in how far state of the art nuclear models can provide reliable answers. In Sec. II we discuss first the Hellmann-Feynman theorem in context with the employed models because the delicate origin of the effect, as explained above, requires models that are variational to achieve sufficient precision. After introducing the nuclear models in Sec. III we discuss in Sec. IV the sensitivity of a temporal drift of fundamental constants like the fine structure constant or the nucleon mass on the transition frequency.

For the nuclear candidate ^{229}Th we perform in Sec. V self-consistent nuclear structure calculations and determine via the Hellmann-Feynman theorem the derivatives of the transition frequency with respect to the fine structure constant and the nucleon mass. A critical assessment is made on the predictive power when calculating observables other than the energy. Finally, we summarize.

II. HELLMANN-FEYNMAN THEOREM REVISITED

In this section we discuss the Hellmann-Feynman theorem for the models we are going to use. As we will see below, the difference of Coulomb energies between ground and excited state of ^{229}Th is about four orders of magnitude smaller than the Coulomb energies themselves. Therefore a precise prediction can only be expected from variational models that fulfill the Hellmann-Feynman theorem.

Let the Hamiltonian $H(\mathbf{c})$ depend on a set of external parameters $\mathbf{c} = \{c_1, c_2, \ldots\}$, like the strength of an interaction or the mass of the particles. The steady-state solutions of the time-dependent Schrödinger equation are given by the eigenvalue problem

$$H(\mathbf{c})|\Psi_n;\mathbf{c}\rangle = E_n(\mathbf{c})|\Psi_n;\mathbf{c}\rangle. \tag{3}$$

Both, the energies $E_n(\mathbf{c})$ and the eigenstates $|\Psi_n;\mathbf{c}\rangle$ depend on $\mathbf{c}$. When discussing intermolecular forces in 1933 H. Hellmann [20] and later in 1939 R. P. Feynman [21] showed that a small variation of an external parameter in the Hamiltonian (distance between nuclei) leads to a change in the energy given by:

$$\frac{\partial}{\partial c_i} E_n(\mathbf{c}) = \frac{\langle\Psi_n;\mathbf{c}|\frac{\partial}{\partial c_i}H(\mathbf{c})|\Psi_n;\mathbf{c}\,\rangle}{\langle\Psi_n;\mathbf{c}|\Psi_n;\mathbf{c}\rangle}. \tag{4}$$

The proof hinges on $|\Psi_n;\mathbf{c}\rangle$ being an eigenstate of the Hermitian $H(\mathbf{c})$.

As was shown in Ref. [22] an analog statement holds for extremal points of an energy functional. Let $\mathcal{E}(\mathbf{c},\mathbf{x})$ be the energy of a physical system that depends on external parameters $\mathbf{c}$ and on a set of variational parameters $\mathbf{x} = \{x_1, x_2, \ldots\}$ that characterize the state of the system. $\mathbf{x}$ may also represent a set of functions in which case partial derivatives are replaced by functional derivatives. For example, in the Hartree-Fock approximation, $\mathbf{x}$ is the set of occupied single-particle states that form a Slater determinant. In an energy density functional $\mathbf{x}$ could be the local density $\rho(\vec{r})$, and so on.

Steady-state solutions $\mathbf{x}^{(n)}(\mathbf{c})$, $n = 0, 1, 2, \ldots$ of the system are obtained by the condition

$$0 = \frac{\partial\mathcal{E}}{\partial x_k}(\mathbf{c},\mathbf{x}). \tag{5}$$

At the stationary points the energy assumes the values

$$E_n(\mathbf{c}) = \mathcal{E}(\mathbf{c},\mathbf{x}^{(n)}(\mathbf{c})), \quad n = 0, 1, 2, \ldots. \tag{6}$$

Both the energies and the parameters $\mathbf{x}^{(n)}(\mathbf{c})$ characterizing the stationary states depend on the constants $\mathbf{c}$. In the ground state given by $\mathbf{x}^{(0)}$ the energy $\mathcal{E}(\mathbf{c},\mathbf{x})$ is in an absolute minimum with respect to variations in $\mathbf{x}$, while the other possible solutions $\mathbf{x}^{(n)}$, $n \neq 0$, represent saddle points.

A variation of the external parameters at the stationary points leads to

$$\delta E_n(\mathbf{c}) = \sum_i \frac{\partial}{\partial c_i} E_n(\mathbf{c})\delta c_i = \sum_i \left\{ \frac{\partial\mathcal{E}}{\partial c_i}(\mathbf{c},\mathbf{x}^{(n)}(\mathbf{c})) + \sum_k \frac{\partial\mathcal{E}}{\partial x_k}(\mathbf{c},\mathbf{x}^{(n)}(\mathbf{c}))\frac{\partial x_k^{(n)}}{\partial c_i}(\mathbf{c}) \right\}\delta c_i. \tag{7}$$

Due to the stationarity condition (5) the second part in the square brackets vanishes so that we obtain for stationary solutions

$$\frac{\partial}{\partial c_i} E_n(\mathbf{c}) = \frac{\partial\mathcal{E}}{\partial c_i}(\mathbf{c},\mathbf{x}^{(n)}(\mathbf{c})). \tag{8}$$

The derivative of the energy at the stationary solutions is just the partial derivative of the energy functional with respect to the external parameter calculated with the stationary state.

III. MODELS

In this section we discuss briefly the Hartree-Fock (HF) method when a Hamiltonian is used, the extension to HF with density-matrix functionals and the inclusion of pairing correlations. We show that in all cases the generalized Hellmann-Feynman relation holds. We also explain in short the quantities discussed in the section containing calculations for ^{229}Th.

A. Hartree-Fock with Hamiltonian

In the HF approximation one uses a single Slater determinant

$$|\Psi_{\rm HF}\rangle = a_1^\dagger a_2^\dagger \cdots a_A^\dagger|\emptyset\rangle \tag{9}$$

as the many-body trial state. The creation operators $a_\nu^\dagger$ that create the occupied single-particle states $|\phi_\nu\rangle$,

$$a_\nu^\dagger|\emptyset\rangle = |\phi_\nu\rangle = \sum_i c_i^\dagger|\emptyset\rangle\, D_{i\nu}, \tag{10}$$

are represented in a working basis $|i\rangle = c_i^\dagger|\emptyset\rangle$. Thus, the expansion coefficients $D_{i\nu}$ represent the set $\mathbf{x} = \{D_{i\nu}; \nu = 1, \ldots, A, i = 1, 2, \ldots\}$ of variational parameters.

The general definition of the one-body density operator

$$\hat{\rho} = \sum_{i,k} |i\rangle\, \rho_{ik}\, \langle k| \tag{11}$$

is given in terms of the expectation values of $c_k^\dagger c_i$, where the creation operators $c_i^\dagger$ create the single-particle basis $|i\rangle$. In the HF case:

$$\rho_{ik} = \frac{\langle\Psi_{\rm HF}|c_k^\dagger c_i|\Psi_{\rm HF}\,\rangle}{\langle\Psi_{\rm HF}|\Psi_{\rm HF}\rangle} = \frac{\sum_\nu D_{i\nu}(D_{k\nu})^*}{\langle\Psi_{\rm HF}|\Psi_{\rm HF}\rangle}. \tag{12}$$

The energy of the HF Slater determinant can be expressed in terms of the idempotent ($\hat{\rho}^2 = \hat{\rho}$) one-body density as

$$\mathcal{E}_{\rm HF}[\mathbf{c}, \hat{\rho}] = \frac{\langle \Psi_{\rm HF}|H(\mathbf{c})|\Psi_{\rm HF}\rangle}{\langle \Psi_{\rm HF}|\Psi_{\rm HF}\rangle} = \sum_{ij} t_{ij}(\boldsymbol{c})\,\rho_{ji} + \frac{1}{4}\sum_{ijkl} v_{ik,jl}(\boldsymbol{c})\rho_{ji}\rho_{lk} + \frac{1}{36}\sum_{ijklmn} v_{ikm,jln}(\boldsymbol{c})\rho_{ji}\rho_{lk}\rho_{nm} + \cdots \quad (13)$$

where $t_{ij}(\mathbf{c})$ denotes the matrix elements of the kinetic energy, $v_{ij,kl}(\mathbf{c})$ the antisymmetrized matrix elements of the two-body interaction, $v_{ikm,jln}(\mathbf{c})$ of the three-body interaction, and so on. The dependence on the parameter set $\mathbf{c}$ that includes the nucleon masses, coupling strengths, interaction ranges, etc., will not be indicated again until required. The variational parameters $\mathbf{x} = \{D_{i\nu}\}$ reside in the one-body density matrix $\hat{\rho}$ as given in Eq. (12). To work with familiar expressions in this section we will write $\hat{\rho}$ instead of $\mathbf{x}$.

Variation of the energy given in Eq. (13) with respect to $\hat{\rho}$ leads to the HF equations

$$\hat{h}_{\rm HF}[\hat{\rho}]\,\hat{\rho} = \hat{\rho}\,\hat{h}_{\rm HF}[\hat{\rho}]. \quad (14)$$

The one-body HF Hamiltonian

$$\hat{h}_{\rm HF}[\hat{\rho}] = \sum_{i,k} |i\rangle\, h_{\rm HF}[\hat{\rho}]_{ik}\,\langle k| \quad (15)$$

is a functional of the one-body density and its matrix elements are given by

$$h_{\rm HF}[\hat{\rho}]_{ik} = \frac{\partial}{\partial \rho_{ki}}\mathcal{E}_{\rm HF}[\mathbf{c}, \hat{\rho}], \quad (16)$$

or in short notation

$$\hat{h}_{\rm HF}[\hat{\rho}] = \frac{\delta}{\delta\hat{\rho}}\mathcal{E}_{\rm HF}[\mathbf{c}, \hat{\rho}]. \quad (17)$$

The eigenstates $|\phi_\nu\rangle$ of $\hat{h}_{\rm HF}[\hat{\rho}]$ represent the basis in which both, $\hat{h}_{\rm HF}[\hat{\rho}]$ and $\hat{\rho}$ are diagonal:

$$\hat{h}_{\rm HF}[\hat{\rho}] = \sum_{\nu} |\phi_\nu\rangle\epsilon_\nu\langle\phi_\nu| \quad (18)$$

$$\hat{\rho} = \sum_{\nu} |\phi_\nu\rangle n_\nu\langle\phi_\nu|, \quad (19)$$

where ϵ_ν denotes the single-particle energy and n_ν are the single-particle occupation numbers that are zero or one in the case of a single Slater determinant. Equation (14) represents the stationarity condition (5) and hence the HF approximation fulfills the Hellmann-Feynman theorem.

In nuclear structure theory the microscopic nucleon-nucleon interaction induces strong short-range correlations that cannot be represented by a single Slater determinant. Therefore the HF method as explained here cannot be used. For example, the strong short-ranged repulsion makes all two-body matrix elements $v_{ik,lm}$ positive and large so the HF Slater determinant does not give bound objects. The way out is to use effective interactions that incorporate the short-range correlations explicitly; see, for example, Ref. [23–25]. Another approach is the density-matrix functional theory we discuss in the following section.

B. Hartree-Fock with density-matrix functionals

It has turned out that bypassing the construction of an effective microscopic Hamiltonian by postulating an ansatz for the energy as functional of the one-body density-matrix $\hat{\rho}$, as originally proposed by Skyrme for the no-relativistic and by J. Boguta and A. R. Bodmer [26] and D. Walecka [27] for relativistic nuclear physics (or by Kohn and Sham [28] for the atomic case), is very successful in describing ground-state properties. The energy functional $\mathcal{E}_{\rm DF}[\mathbf{c}, \hat{\rho}]$ contains a finite number of parameters, $\mathbf{c}$, that are adjusted by fitting observables to nuclear data. The shape of the functional is subject of past and present research [29–31] and is being improved to also apply for nuclei far off stability. Differing from the HF case with Hamiltonian, Eq. (13), the densities may appear also with noninteger powers and the exchange terms are not calculated explicitly but absorbed in the form of the energy functional.

Not all of the information residing in the one-body density-matrix $\hat{\rho}$ is used. Usually one uses the proton and neutron density $\rho_p(\vec{r}), \rho_n(\vec{r})$, kinetic energy densities $\tau_p(\vec{r}), \tau_n(\vec{r})$, current densities $\vec{j}(\vec{r})$, etc.

$$\mathcal{E}_{\rm DF}[\mathbf{c}, \hat{\rho}] = \mathcal{E}_{\rm DF}[\mathbf{c}, \rho_p(\vec{r}), \rho_n(\vec{r}), \tau_p(\vec{r}), \tau_n(\vec{r}), \vec{j}(\vec{r}), \ldots]. \quad (20)$$

To keep densities and currents consistent and corresponding to fermions they are expressed in terms of the single-particle states $|\phi_\nu\rangle$

$$|\phi_\nu\rangle = \sum_i |i\rangle\, D_{i\nu} \quad (21)$$

that represent the occupied states of a single Slater determinant. As they are expanded in terms of a working basis $|i\rangle$ the energy $\mathcal{E}_{\rm DF}[\mathbf{c}, \hat{\rho}]$ is, like in the HF case, a function of the variational parameters $\mathbf{x} = \{D_{i\nu}; i, \nu = 1, 2, \ldots\}$ or $\mathbf{x} = \hat{\rho}$.

The difference to HF with a Hamiltonian is that the mean-field Hamiltonian $\hat{h}_{\rm MF}[\hat{\rho}]$ obtained by the functional derivative of the density-matrix functional $\mathcal{E}_{\rm DF}$

$$\hat{h}_{\rm MF}[\hat{\rho}] = \frac{\delta}{\delta\hat{\rho}}\mathcal{E}_{\rm DF}[\mathbf{c}, \hat{\rho}] \quad (22)$$

is no longer given by a microscopic Hamiltonian but rather by the functional form of $\mathcal{E}_{\rm DF}$ and the fitted parameters in the set $\mathbf{c}$.

The stationarity conditions (5) lead to the self-consistent mean-field equations

$$\hat{h}_{\rm MF}[\hat{\rho}]\,\hat{\rho} = \hat{\rho}\,\hat{h}_{\rm MF}[\hat{\rho}] \quad (23)$$

that have the same structure as the HF equations.

Because the self-consistent solution is obtained by searching for solutions of the stationarity conditions (5), the Hellmann-Feynman theorem (8) is fulfilled, even if one can no longer refer to a microscopic Hamiltonian and a many-body state.

One should note that it is not mandatory that the single-particle states $|\phi_\nu\rangle$ with lowest single-particle energies are occupied. Any combination of occupied states leads to a stationary solution fulfilling Eq. (23).

Another interesting case is a one-body density with fractional occupation numbers $0 \leqslant n_\nu \leqslant 1$ that may also commute with the mean-field Hamiltonian and hence fulfills the stationarity condition (23) so the Hellmann-Feynman theorem is applicable. In such a situation one cannot attribute a single Slater determinant to the one-body density, because $\hat{\rho} \neq \hat{\rho}^2$ is not idempotent.

In any case the occupation numbers play the role of external parameters and should be regarded as members of the set **c** and not as variational parameters.

C. Hartree-Fock-Bogoliubov

The solution of the eigenvalue problem of $\hat{h}_{\rm MF}[\hat{\rho}]$ provides not only the coefficients $D_{i\nu}$ of the occupied single-particle states but also a representation for empty states so that one has a complete representation of the one-body Hilbert space. With that one can define creation operators for fermions for occupied and empty states

$$a_\nu^\dagger = \sum_i c_i^\dagger\, D_{i\nu}, \tag{24}$$

with

$$|\phi_\nu\rangle = a_\nu^\dagger|\emptyset\rangle \quad \text{and} \quad |i\rangle = c_i^\dagger|\emptyset\rangle. \tag{25}$$

and their corresponding annihilation operators a_ν and c_i.

Pairing correlations in the many-body state can be incorporated by Bogoliubov quasiparticles that are created by

$$\begin{aligned} \alpha_\nu^\dagger &= u_\nu a_\nu^\dagger - v_\nu a_{\bar{\nu}} \\ \alpha_{\bar{\nu}}^\dagger &= u_\nu a_{\bar{\nu}}^\dagger + v_\nu a_\nu \end{aligned} \tag{26}$$

as linear combinations of the creation and annihilation operators, $a_\nu^\dagger, a_{\bar{\nu}}$, of the eigenstates of the one-body density matrix (the so-called canonical states). The parameters u_ν and v_ν can be chosen real and the requirement that $\alpha_\nu^\dagger$ and $\alpha_{\bar{\nu}}^\dagger$ are fermionic quasiparticle operators implies $u_\nu^2 + v_\nu^2 = 1$. The pairing partner states ν and $\bar{\nu}$ are usually mutually time-reversed states.

The many-body trial state is expressed as

$$|\Psi_{\rm HFB}\rangle = \prod_\mu a_\mu^\dagger \prod_\nu \left(\sqrt{1 - v_\nu^2} + v_\nu\, a_\nu^\dagger a_{\bar{\nu}}^\dagger\right)|\emptyset\rangle, \tag{27}$$

where the product over μ runs over the so-called blocked states or unpaired states and ν runs over all other paired states. In addition to the variational parameters residing in the operators $a_\nu^\dagger$ that create eigenstates of the mean-field Hamiltonian the energy depends now also on the variational parameters v_ν, hence $\mathbf{x} = \{D_{i\nu}, v_\nu; i, \nu = 1, 2, \ldots\}$.

As the trial state (27) has no sharp particle number the stationarity conditions Eq. (5) have to be augmented by a constraint on mean proton number $\mathcal{Z}$ and mean neutron number $\mathcal{N}$ to obtain the self-consistent Hartree-Fock-Bogoliubov (HFB) equations:

$$\mathcal{E}_{\rm HFB} = \mathcal{E} - \lambda_p \mathcal{Z} - \lambda_n \mathcal{N}. \tag{28}$$

The proton and neutron chemical potentials, λ_p and λ_n, have to be regarded as members of the set $\boldsymbol{c}$ of external parameters. The additional constraints do not alter the arguments leading the Hellmann-Feynman theorem [22], thus it is also valid in the HFB case.

In HFB it is convenient to introduce a generalized density matrix

$$\widehat{\mathcal{R}} = \begin{pmatrix} \hat{\rho} & \hat{\kappa} \\ -\hat{\kappa}^* & 1 - \hat{\rho}^* \end{pmatrix}, \tag{29}$$

where $\hat{\rho}$ is the normal one-body density

$$\rho_{ik} = \frac{\langle \Psi_{\rm HFB}|c_k^\dagger c_i|\Psi_{\rm HFB}\rangle}{\langle \Psi_{\rm HFB}|\Psi_{\rm HFB}\rangle} \tag{30}$$

and κ the so-called abnormal density

$$\kappa_{ik} = \frac{\langle \Psi_{\rm HFB}|c_k c_i|\Psi_{\rm HFB}\rangle}{\langle \Psi_{\rm HFB}|\Psi_{\rm HFB}\rangle}. \tag{31}$$

Both can be expressed in terms of $D_{i\nu}$ and v_ν. The generalized density matrix is idempotent and Hermitian

$$\widehat{\mathcal{R}}^2 = \widehat{\mathcal{R}} \quad \text{and} \quad \widehat{\mathcal{R}}^\dagger = \widehat{\mathcal{R}} \tag{32}$$

and the stationarity condition leads to

$$\widehat{\mathcal{H}}_{\rm MF}[\widehat{\mathcal{R}}]\,\widehat{\mathcal{R}} = \widehat{\mathcal{R}}\,\widehat{\mathcal{H}}_{\rm MF}[\widehat{\mathcal{R}}] \tag{33}$$

quite in analogy to the mean-field equations (23) without pairing correlations. The pseudo-Hamiltonian

$$\widehat{\mathcal{H}}_{\rm MF}[\widehat{\mathcal{R}}] = \frac{\delta}{\delta \widehat{\mathcal{R}}} \mathcal{E}_{\rm HFB}[\boldsymbol{c}, \widehat{\mathcal{R}}] = \begin{pmatrix} \hat{h}_{\rm MF} - \lambda & \hat{\Delta} \\ -\hat{\Delta}^* & \lambda - \hat{h}_{\rm MF}^* \end{pmatrix} \tag{34}$$

contains the mean-field Hamiltonian and the pairing part $\hat{\Delta}$. The chemical potentials $\lambda = (\lambda_p, \lambda_n)$ determine the mean proton and neutron number. For details and further reading see Refs. [32–34].

Let us write down only the one-body density because it is referred to in the results for ^{229}Th. The one-body density matrix is given by

$$\hat{\rho} = \sum_{\nu\ \text{paired}} |\phi_\nu\rangle v_\nu^2 \langle \phi_\nu| + \sum_{\mu\ \text{blocked}} |\phi_\mu\rangle n_\mu \langle \phi_\mu|, \tag{35}$$

where the $|\phi_\nu\rangle$ denote canonical basis states. The occupation numbers are given by $n_\nu = n_{\bar{\nu}} = v_\nu^2$ for the paired states and are the same for ν and $\bar{\nu}$. For the unpaired or blocked states $n_\mu = 0, 1$. In the application we will consider only one blocked neutron state for ^{229}Th.

IV. SENSITIVITY

To be more specific let us consider as external parameters the fine structure constant α and the proton and neutron mass m_p, m_n, thus $\mathbf{c} = \{\alpha, m_p, m_n\}$. In this section, we write down expressions pertaining to a Hamiltonian; those characteristic to a density functional are entirely analogous, cf. Sec. II. The partial derivatives of a nonrelativistic Hamiltonian are

$$\frac{\partial}{\partial\alpha}H(\alpha, m_p, m_n) = \frac{1}{\alpha}V_C \tag{36}$$

$$\frac{\partial}{\partial m_p}H(\alpha, m_p, m_n) = Z - \frac{1}{m_p}T_p \tag{37}$$

$$\frac{\partial}{\partial m_n}H(\alpha, m_p, m_n) = N - \frac{1}{m_n}T_n, \tag{38}$$

where V_C denotes the operator for the Coulomb energy, Z, N the proton and neutron number, respectively, and T_p, T_n stand for the proton and neutron kinetic energy operator, respectively.

According to the Hellmann-Feynman theorem a small variation $\delta\alpha$ of the fine structure constant results in a variation of an energy eigenvalue given by

$$\delta E_n = \Bigg(\langle\Psi_n|V_C|\Psi_n\rangle + Z\,\alpha\frac{dm_p}{d\alpha} + N\,\alpha\frac{dm_n}{d\alpha} - \langle\Psi_n|T_p|\Psi_n\rangle\frac{\alpha\frac{dm_p}{d\alpha}}{m_p} - \langle\Psi_n|T_n|\Psi_n\rangle\frac{\alpha\frac{dm_n}{d\alpha}}{m_n}\Bigg)\frac{\delta\alpha}{\alpha}. \tag{39}$$

In principle there could also be a dependence of the nuclear interaction V_N on α, e.g., through meson masses, which we neglect here. The dependence of the nucleon masses on α can be estimated from the article by Meißner *et al.* [35] [Eq. (36)]. Their estimate of the neutron-proton mass difference due to the electromagnetic interaction is $\Delta m_{np}^{(\mathrm{EM})} = -0.68$ MeV that yields

$$\begin{aligned}\frac{\alpha\frac{dm_p}{d\alpha}}{m_p} &= -\frac{\Delta m_{np}^{(\mathrm{EM})}}{2m_p} \approx +0.36\times10^{-3}\\ \frac{\alpha\frac{dm_n}{d\alpha}}{m_n} &= \frac{\Delta m_{np}^{(\mathrm{EM})}}{2m_n} \approx -0.36\times10^{-3}.\end{aligned} \tag{40}$$

A possible variation of some QCD constant c would lead to

$$\delta E_n = \Bigg(\langle\Psi_n|\frac{d}{dc}V_N(c)|\Psi_n\rangle + Z\,\frac{dm_p}{dc} + N\,\frac{dm_n}{dc} - \langle\Psi_n|T_p|\Psi_n\rangle\frac{\frac{dm_p}{dc}}{m_p} - \langle\Psi_n|T_n|\Psi_n\rangle\frac{\frac{dm_p}{dc}}{m_n}\Bigg)\delta c \tag{41}$$

where V_N is the nuclear part of the interaction. This variation is actually linked to the dimensionless ratio $c = m_q/\Lambda_{\mathrm{QCD}}$, where m_q denotes the current quark mass and Λ_{QCD} the strong interaction scale [11,36,37].

While the dependence of the nucleon mass on the current quark mass has been calculated [38,39], the QCD constants enter the effective interaction $V_N(c)$ in a very complicated and yet unknown way. In this article we do not consider such variations of QCD constants explicitly but calculate besides the total energies the kinetic energies and the Coulomb energies that then can be combined according to Eqs. (39) or (41) to obtain the variations with respect to variations of α or QCD parameters.

As the temporal variation of the fundamental constant α is tiny, if existent, it has been proposed to consider transition frequencies

$$\nu = \frac{1}{h}[E_1(\alpha) - E_0(\alpha)] \tag{42}$$

that can be measured with high precision.

If the two energy levels belong to the same nucleus the terms with the proton and neutron number drop out and we obtain for the change $\delta\nu$ of the transition frequency

$$\begin{aligned}\delta\nu &= \frac{1}{h}\left(\frac{\partial E_1}{\partial\alpha} - \frac{\partial E_0}{\partial\alpha}\right)\delta\alpha\\ &= \left(\frac{\Delta V_C}{h} - \frac{\Delta T_p}{h}\frac{\alpha\frac{dm_p}{d\alpha}}{m_p} - \frac{\Delta T_n}{h}\frac{\alpha\frac{dm_n}{d\alpha}}{m_n}\right)\frac{\delta\alpha}{\alpha}\end{aligned} \tag{43}$$

with the abbreviation

$$\Delta X = \frac{\langle\Psi_1;\alpha|X|\Psi_1;\alpha\rangle}{\langle\Psi_1;\alpha|\Psi_1;\alpha\rangle} - \frac{\langle\Psi_0;\alpha|X|\Psi_0;\alpha\rangle}{\langle\Psi_0;\alpha|\Psi_0;\alpha\rangle} \tag{44}$$

for the difference of the expectation values of the operators $X = \{V_C, T_p, T_n\}$ calculated with the stationary states. The terms in the bracket in Eq. (43) represent the sensitivities [19] with respect to variations of α.

The results discussed in Sec. V show that ΔT_n and ΔT_p are of the same order as ΔV_C, nevertheless the terms with the proton and neutron mass variations can be neglected because of the very small variations of the nucleon masses with respect to α, see Eq. (40).

When measuring frequencies one has to refer to a clock, for example, the Cs fountain clock. The temporal shift in frequency ν with respect to the clock frequency ν_c due to temporal changes in α can be written as [7,8]

$$\frac{\partial}{\partial t}\ln\frac{\nu}{\nu_c} = (A - A_c)\frac{\partial}{\partial t}\ln\alpha, \tag{45}$$

where $A = q_s/\nu$ denotes relative sensitivities. For measured atomic transitions $A - A_c$ is typically of order one. The nuclear case of ^{229}Th [10,11] has attracted a lot of interest as the relative sensitivity $A = \Delta V_C/(h\nu)$ could potentially be of order 10^4 that would improve the limit on temporal changes of α substantially, as discussed in the introduction.

To confirm this the frequency ν has to be measured and the theoretical task is to investigate the nuclear states carefully to get a reliable estimate for their Coulomb and kinetic energies. For the calculation of these quantities we employ in the following section state-of-the-art mean-field models and also include the effects of pairing correlations.

V. RESULTS FOR ^{229}Th

The nucleus ^{229}Th with 90 protons and 139 neutrons occurs in nature as the daughter of the α-decaying ^{233}U and decays itself with a half-life of 7880 years, again by α emission. This nucleus has attracted lot of interest as it has the lowest-lying excited state known. In Fig. 1 the spectrum is arranged in terms of rotational bands [40]. Two low-lying rotational bands with $K^\pi = 5/2^+$ and $3/2^+$ can be identified, with band heads that according to recent measurements differ in energy by only about 8 eV. The first negative-parity band with $K^\pi = 5/2^-$ occurs at 146.36 keV.

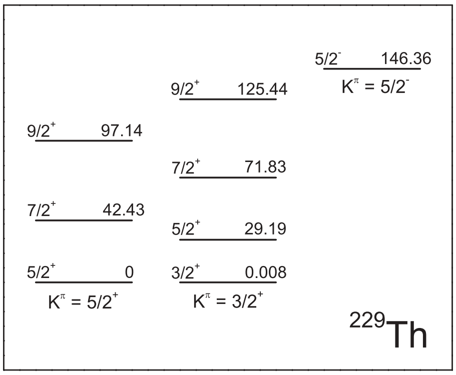

FIG. 1. Measured low lying states of ^{229}Th with spin and parity assignments [40]. Energies are in keV.

Because of the high sensitivity discussed in Sec. IV the transition $3/2^+ \rightarrow 5/2^+$ is regarded as a possible candidate to measure the time variation of the fine structure constant. A simple estimate of the moment of inertia for the two bands assuming a $J(J+1)$ energy dependence shows that the two rotational bands have very similar intrinsic deformation. Therefore, one does not expect a large difference between the Coulomb energies of the $5/2^+$ and $3/2^+$ band heads that would be due to differences in shapes. Instead, one has to consider and work out detailed effects due to different configurations of these states.

A. Hartree-Fock with density-matrix functional theory

To come to more quantitative statements we calculate the energies of these two states with the best methods available: density-matrix functional theory without and with pairing, and a spherical relativistic mean-field theory [41]. In the nonrelativistic case we use the computer program HFODD (v2.33j) [42,43] and employ two successful energy functionals, SIII [44] and SkM* [45]. Because of large uncertainties related to polarization effects due to time-odd mean fields [46], in the present study these terms in the energy functionals are neglected. The standard Slater approximation is used to calculate the Coulomb exchange energies. The code works with Cartesian harmonic oscillator (HO) eigenstates as working basis $|i\rangle$ and allows for triaxial and parity-breaking deformations, but the states determined in ^{229}Th turn out to have axial shapes with conserved parity. In our calculations we have used the basis of HO states up to the principal quantum number of $N_0 = 18$ and the same HO frequency of $\hbar\omega = 8.05$ MeV in all three Cartesian directions.

In the discussion, the resulting basis $|\phi_\nu\rangle$ will be assigned Nilsson quantum numbers $\Omega^\pi[N, N_z, \Lambda]$ (for details see Ref. [32,47]) by looking for the largest overlap $|\langle\Omega^\pi[N, N_z, \Lambda]|\phi_\nu\rangle|$ with a Nilsson state. $N = N_x + N_y + N_z = N_\rho + N_z + \Lambda$ denotes the total number of oscillator quanta and N_z the number of quanta in the direction of the symmetry axis. $\Lambda = N_\rho, N_\rho - 2, \ldots 0$ or 1 and $\Omega = \Lambda \pm \frac{1}{2}$ are the absolute values of the projection of orbital angular momentum and total spin on the symmetry axis, respectively. $\pi = (-1)^N$ is the parity.

It turns out that for both functionals the lowest HF state has $\Omega^\pi = 5/2^-$ and thus corresponds to the intrinsic state of the $K^\pi = 5/2^-$ band that is experimentally located at 146.36 keV. The total binding energy amounts to -1739.454 MeV for SkM* and -1741.885 MeV for SIII that should be compared to the experimental energy of -1748.334 MeV [40]. On this absolute scale the calculated HF energies are already amazingly good.

To get the experimentally observed parity we perform the variation procedure in the subspace with positive parity. For both energy functionals the Slater determinant with the lowest energy has $K^\pi = 5/2^+$. All energies are summarized in Table I. The last neutron occupies the level labeled with $5/2^+[622]$ in the SkM* and with $5/2^+[633]$ in the SIII case. One should keep in mind that the single-particle states are superpositions of Nilsson states and the labeling refers only to the largest component. The states are detailed in Eqs. (46)–(49) below.

The neutron single-particle energies ϵ_ν and the occupation numbers are displayed in Fig. 2(a) for SkM* and in Fig. 3(a) for SIII. The $5/2^-[752]$ state that would be occupied in the negative-parity case is very close to the $5/2^+[633]$ state; for SIII they are almost degenerate.

As can be seen from Table I, the total HF binding energy agrees with the measured one up to about 9 MeV for the SkM* and up to about 6 MeV for the SIII energy functional. Keeping in mind that no parameters have been adjusted to the specific nucleus considered here it is surprising that these mean-field models can predict the energy with an uncertainty of only about 0.5 %.

Putting two neutrons in the $5/2^+[622]$ (for SkM*) or $5/2^+[633]$ (for SIII) level and one in the $3/2^+[642]$ (for SkM*) or $3/2^+[631]$ (for SIII) level and minimizing the total energy yields an excited HF state that is to be regarded as the intrinsic state of the experimentally observed $K^\pi = 3/2^+$ band. As can be seen in Table I, the excited states occur at 0.619 MeV for the SkM* and at 0.141 MeV for the SIII density functional. The difference in Coulomb energies ΔV_C amounts to 0.451 MeV for SkM* and to -0.098 MeV for SIII. The kinetic energy differences ΔT_p and ΔT_n for protons and neutrons, respectively, dissent even more. These deviations between the two energy functionals reflect the differences in the structure of the intrinsic states as also seen from the difference in the single-particle states discussed above.

B. Relativistic mean-field calculation

We also performed a spherical relativistic mean-field calculation with the NL3 parameter set [48] and found that in the ground state the last neutron occupies a $2g_{9/2}$ orbit. For vanishing deformation the Nilsson state $5/2^+[633]$ belongs to the subspace spanned by the spherical $2g_{9/2}$ orbits so that this result is not unreasonable when comparing with the deformed SIII calculation. The leading component for the $3/2^+$ state is for SIII the $3/2^+[631]$ orbit (cf. Fig. 3) that for deformation zero belongs to the $1i_{11/2}$ subshell. Therefore we create the excited state with $\Omega^\pi = 3/2^+$ by a particle-hole excitation from the $1i_{11/2}$ to the $2g_{9/2}$ shell so that there are 11 neutrons in the $1i_{11/2}$ and 2 neutrons in the $2g_{9/2}$ shell.

TABLE I. Total, Coulomb, neutron, and proton kinetic energies of the ^{229}Th $5/2^+$ ground state calculated with different energy functionals. Differences of these energies between $3/2^+$ first excited state and $5/2^+$ ground state.

	Exp.	SkM*		SIII		NL3 RH
		HF	HFB	HF	HFB	
$5/2^+$	Ref. [40]					
E^{tot} (MeV)	−1748.334	−1739.454	−1747.546	−1741.885	−1748.016	−1745.775
V_C (MeV)		923.927	924.854	912.204	912.216	948.203
T_n (MeV)		2785.404	2800.225	2783.593	2794.909	2059.640
T_p (MeV)		1458.103	1512.705	1442.018	1477.485	1106.697
$3/2^+ - 5/2^+$	Ref. [12]					
ΔE^{tot}(MeV)	0.000 008	0.619	−0.046	0.141	−0.074	2.407
ΔV_C (MeV)		0.451	−0.307	−0.098	0.001	1.011
ΔT_n (MeV)		2.570	0.954	−0.728	0.087	−2.181
ΔT_p (MeV)		0.688	0.233	−0.163	−0.022	−1.996

The resulting energies are listed in the last column of Table I. The total binding energy is similar to the nonrelativistic one, but the particle-hole excited state is 2.41 MeV higher. Different from the deformed mean-field the single-particle states of a spherical potential have good total spin j and are $(2j+1)$-fold degenerated with large gaps between them. The single-particle energy difference $\epsilon_{9/2} - \epsilon_{11/2} = 2.74$ MeV explains the large excitation energy of the particle-hole pair of 2.41 MeV, which includes the rearrangement energy.

We conclude that a spherical calculation is not appropriate for this particular question. In a recent publication [49] a similar spherical relativistic mean-field calculations comes to results comparable to ours with a Coulomb energy difference of 0.7 MeV. Because of the unphysical properties of a spherical ^{229}Th we will not commit ourselves to the spherical case any longer but proceed to consider the effects of pairing.

C. Hartree-Fock-Bogoliubov

We include the pairing correlations with the Bogoliubov ansatz (27) and perform a self-consistent HFB calculation based on the SkM* and SIII density-matrix functional. For the SIII case proton and neutron pairing strengths of $V_0 = -260$ and -180 MeV fm^3 (for a volume-type contact force) are adjusted to reproduce the total binding energies and the odd-even staggering with the neighboring nuclei. Proton- and neutron-density matrices and pairing tensors are calculated by including contributions from quasiparticle states up to the cutoff energy of 60 MeV. Calculations are performed by self-consistently blocking the $5/2^+$ and the $3/2^+$ quasiparticle states. In the $5/2^+$ and $3/2^+$ configurations, this yields the average HFB proton and neutron pairing gaps of $\Delta_p = 2.4$ MeV and $\Delta_n = 0.65$ MeV, and $\Delta_p = 2.4$ MeV and $\Delta_n = 0.68$ MeV, respectively, for the SIII case and slightly larger values for the SkM* case.

The results for the energies are summarized in Table I and for the mean-field single-particle energies and the occupation probabilities in Fig. 2(b) and Fig. 3(b). The first to note is that the excitation energy is improving. Its value decreases from 619 keV down to −46 keV for SkM* and from 141 keV down to −74 keV for SIII. On the accuracy level one can expect from this model the $5/2^+$ and the $3/2^+$ states are degenerate, like in experiment.

By looking at the occupation numbers displayed in Figs. 2(b) and 3(b) one sees that about five single particle levels near the Fermi edge assume fractional occupation numbers significantly different than 0 or 2. In the SIII case [Fig. 3(b)] they are almost identical for the $5/2^+$ and $3/2^+$ states except for the $5/2^+[633]$ and $3/2^+[631]$ levels that switch their role. For the SkM* case [Fig. 2(b)] the blocked states are energetically further away from each other, which causes more deviations in the occupation numbers.

This characteristic pattern of occupation numbers renders the HFB results qualitatively different than the HF ones. Indeed, in the HF case either the $5/2^+$ or the $3/2^+$ orbital has the occupation number equal to 1. Therefore, polarization effects exerted by these two orbitals are able to render different values of observables calculated for the $5/2^+$ and $3/2^+$ states. In the HFB case, occupation numbers of the $5/2^+$ and $3/2^+$ orbitals are close to 1 for both $5/2^+$ and $3/2^+$ configurations. Differences in observables may here only occur due to the fact that the occupation number of the blocked state is exactly equal to 1, while that of the other state is approximately equal to 1, depending on its closeness to the Fermi level.

In the paired case (HFB), we are faced with the situation, where the zero-order approximation renders observables calculated in the $5/2^+$ and $3/2^+$ exactly equal. Indeed, such equality would be the case for the $5/2^+$ and $3/2^+$ orbitals located exactly at the Fermi surface and having exactly the same occupation numbers. Note that values of all observables calculated with the HFB approach depend only on the canonical states and occupation numbers, irrespective of which state has been blocked in obtaining them. Of course, one can obtain different occupation numbers for both orbitals in question when they are energetically split. However, this may contradict the experimental energetic degeneracy of the corresponding configurations. All in all, within a zero-order paired approach, polarization effects of the $5/2^+$ and $3/2^+$ orbitals become exactly averaged out and the anticipated differences in observables can occur only due to first-order corrections.

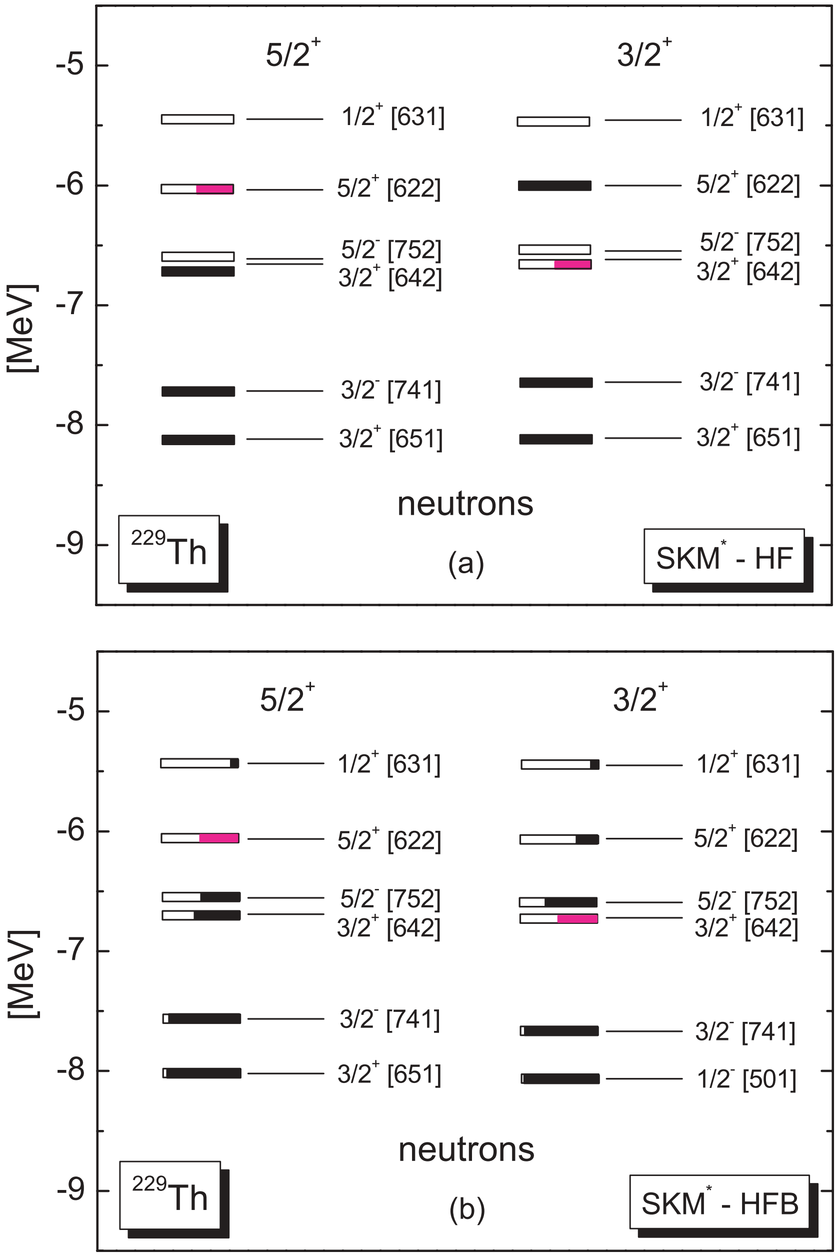

FIG. 2. (Color online) Neutron single-particle energies and occupation numbers labeled by the asymptotic Nilsson quantum numbers $\nu = \Omega^\pi[N, N_z, \Lambda]$ for the SkM* energy functional. (a) HF mean-field energies ϵ_ν and occupation numbers n_ν. Full bars denote $n_\nu + n_{\bar\nu} = 2$, i.e., two particles in degenerate pair of states with $m_j = \pm\Omega$. Half full gray (pink) bars denote one particle, $n_\mu = 1,\ n_{\bar\mu} = 0$. (b) HFB mean-field energies ϵ_ν (eigenvalues of $\hat h_{\mathrm{MF}}$) and occupation numbers v_ν^2. Length of bars indicates $n_\nu + n_{\bar\nu}$. Gray (pink) bars stand for blocked states with $n_\mu = 1,\ n_{\bar\mu} = 0$.

This fact is perfectly well visible in our results for the Coulomb energy differences shown in Table I. For the SIII energy functional, only 1 keV remains for ΔV_C. This reduces the sensitivity of Eq. (43) to about 10^{17}Hz. For SkM* a larger value of ΔV_C of about 300 keV is obtained due to a larger splitting of the corresponding single-particle orbitals. From this one must conclude that pairing correlations result in two states with even more similar charge distributions than in the HF calculation.

D. Radii and quadrupole moments

In Table II the rms-radii and quadrupole moments (normalized with proton and neutron number, respectively) of the neutron and proton point densities are given for the ground state and as differences for the excited state. The quadrupole moments of the protons are somewhat larger than those for the neutrons. When reoccupying the last neutron the neutron quadrupole moment decreases substantially in the SkM*-HF calculation and drags along via the nuclear interaction the quadrupole moment of the protons. At the same time both rms radii are decreased. A smaller charge radius and smaller charge quadrupole moment are consistent with the increase of the Coulomb energy that explains the large positive ΔV_C in the SkM*-HF case. When including pairing the effect goes in the opposite direction for SkM*-HFB.

For the SIII functional HF and HFB calculations do not lead to noteworthy changes in the moments when reoccupying the last neutron and thus the Coulomb differences remain also small. This can be anticipated when looking at the single-particle energies of the involved neutron states and the occupation numbers (Fig. 3).

TABLE II. Rms-radius and intrinsic quadrupole moments of neutron and proton densities of the ^{229}Th $5/2^+$ ground state calculated with different energy functionals. Differences of these moments between $3/2^+$ first excited state and $5/2^+$ ground state.

	SkM*		SIII	
	HF	HFB	HF	HFB
$5/2^+$				
$R_{\rm rms}$(neutron) (fm)	5.8789	5.8716	5.8971	5.8923
$R_{\rm rms}$(proton) (fm)	5.7180	5.7078	5.7817	5.7769
Q_{20} (neutron) (fm^2)	9.4407	9.2608	9.1990	9.0711
Q_{20} (proton) (fm^2)	9.5461	9.3717	9.3542	9.1643
$3/2^+ - 5/2^+$				
$\Delta R_{\rm rms}$(neutron) (fm)	−0.0040	0.0036	−0.0008	−0.0005
$\Delta R_{\rm rms}$(proton) (fm)	−0.0038	0.0039	0.0000	−0.0005
ΔQ_{20} (neutron) (fm^2)	−0.2427	0.2647	−0.0767	−0.0516
ΔQ_{20} (proton) (fm^2)	−0.1824	0.2756	−0.0339	−0.0495

The mean-field single-particle state that corresponds to the blocked HFB state occupied by the unpaired neutron is represented in Nilsson orbits for SkM*-HF as

$$\begin{aligned}\left|\tfrac{5}{2}^+\right\rangle &= +.509|622\rangle + .467|642\rangle + .266|862\rangle \\ &\quad + .402|633\rangle - .397|613\rangle + \cdots \\ \left|\tfrac{3}{2}^+\right\rangle &= -.010|622\rangle + .662|642\rangle + .249|862\rangle \\ &\quad + .305|611\rangle - .562|631\rangle + \cdots\end{aligned} \tag{46}$$

and for SkM*-HFB including pairing as

$$\begin{aligned}\left|\tfrac{5}{2}^+\right\rangle &= +.504|622\rangle + .487|642\rangle + .248|862\rangle \\ &\quad + .418|633\rangle - .383|613\rangle + \cdots \\ \left|\tfrac{3}{2}^+\right\rangle &= +.015|622\rangle + .642|642\rangle + .235|862\rangle \\ &\quad + .305|611\rangle - .582|631\rangle + \cdots .\end{aligned} \tag{47}$$

The SIII-HF calculation gives

$$\begin{aligned}\left|\tfrac{5}{2}^+\right\rangle &= +.066|622\rangle + .418|642\rangle + .180|862\rangle \\ &\quad + .755|633\rangle - .398|613\rangle + \cdots \\ \left|\tfrac{3}{2}^+\right\rangle &= +.134|622\rangle + .360|642\rangle + .165|862\rangle \\ &\quad + .428|611\rangle - .642|631\rangle + \cdots\end{aligned} \tag{48}$$

and the SIII-HFB with pairing

$$\begin{aligned}\left|\tfrac{5}{2}^+\right\rangle &= +.024|622\rangle + .423|642\rangle + .159|862\rangle \\ &\quad + .775|633\rangle - .367|613\rangle + \cdots \\ \left|\tfrac{3}{2}^+\right\rangle &= +.156|622\rangle + .342|642\rangle + .149|862\rangle \\ &\quad + .412|611\rangle - .636|631\rangle + \cdots .\end{aligned} \tag{49}$$

In SIII-HF and SIII-HFB the blocked states exhibit more concentration on the dominant Nilsson orbits [633] and [631]. As both have the same nodal structure in z direction ($N_z = 3$) one expects less difference in the density distribution than in the SkM* case where both states are superpositions of several Nilsson orbits with similar amplitudes. In the SkM* case the leading component of $|\frac{5}{2}^+\rangle$ is [622] and of $|\frac{3}{2}^+\rangle$ is [642], which implies a change in nodal structure in the z direction. In summary the polarization of the proton distribution due to the reoccupation of the level with the unpaired neutron has less effect in the SIII than in the SkM* case.

In Ref. [50] the finite-range microscopic-macroscopic model has been used to study the problem. The authors find small Coulomb energy differences similar to our SIII case. Also the decomposition of the last neutron orbits[1] shows a mixture of several Nilsson orbits resembling more our SIII states than the SkM* states.

We should like to point out that the Nilsson orbit $5/2^+[633]$ that is usually used to classify the $K^\pi = 5/2^+$ ground-state band [12,51–53] does not even contain a single-particle spin $j^\pi = 5/2^+$. Due to positive parity and $\Lambda = |m_l| = 3$ the orbital angular momenta contained in $5/2^+[633]$ are $l = 4, 6, \ldots$. Thus the lowest possible spin in the $5/2^+[633]$ Nilsson state is $j^\pi = 7/2^+$. This implies that in a core plus valence-neutron picture the $5/2^+[633]$ state needs to be coupled to the excited $J^\pi = 2^+$ state in ^{228}Th to get the ground-state spin $J^\pi = 5/2^+$. In the deformed mean-field description the total angular momentum $J^\pi = 5/2^+$ of the nucleus arises from both the $5/2^+[633]$ orbital and the underlying deformed ^{228}Th core.

In Refs. [51,53,54] detailed experimental data have been compared with structure calculations for ^{229}Th that use the quasiparticle-phonon model (QPM) [55] employing a phenomenological Nilsson mean field and multipole-multipole residual interactions. A very good description of the ^{229}Th level structure has been achieved by an appropriate fit of the interaction parameters. It has, for example, been found that the coupling of the single-quasiparticle degrees of freedom to the collective octupole vibrational state of the ^{228}Th core is essential to reproduce the parity partner bands observed in experiment. Despite its success the QPM is not self-consistent and thus cannot be used for our considerations. But the insight gained with QPM should be a guide for future variational models that have to treat higher-order correlations in a self-consistent way.

In a fully consistent calculation scheme based on a relativistic density-matrix functional [56] it has been shown that the coupling to low lying vibrations noticeably improves the description of the single-particle spectrum around the Fermi surface, including the ordering of the levels. This model is, however, programed only for spherical cases.

One has to realize that the situation is not so simple. Valence and core nucleons have to be considered self-consistently and in the next generation of nuclear models, in addition to the projection of the deformed intrinsic state on total spin and particle number, one also may need to go beyond the mean-field picture by coupling to low-lying core excitations.

E. Predictive power and accuracy of observables

In the energy-density functional picture one gives up the explicit knowledge of a microscopic Hamilton operator $H(\boldsymbol{c})$

[1]Please note that in Ref. [50] the authors seem to have mixed up the right hand sides of Eqs. (1) and (2).

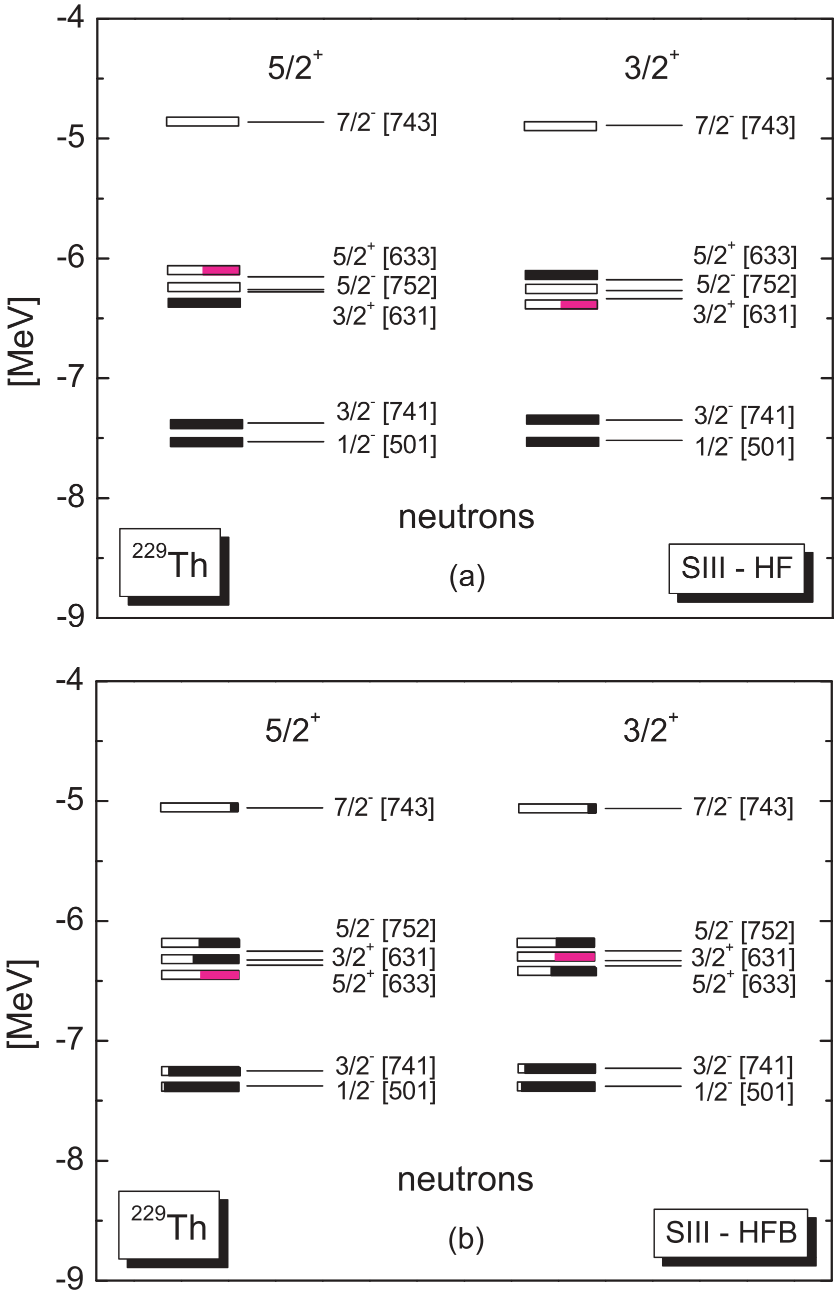

FIG. 3. (Color online) Same as described in the caption to Fig. 2 but for the SIII energy functional.

acting in many-body Hilbert space. Its expectation value is replaced by the energy functional $\mathcal{E}[\mathbf{c}, \hat{\rho}]$ from which one cannot refer back to the Hamiltonian. It is important to note that one can also not refer back to a many-body state $|\Psi\rangle$ that represents an approximation to a true stationary eigenstate of $H(\boldsymbol{c})$. One can, of course, construct a single Slater determinant with the operators $a_\nu^\dagger$ that, which create the occupied states, but this Slater determinant is more an auxiliary object that ensures quantum properties like Pauli principle or uncertainty relation. This Slater determinant misses for example various kinds of typical nuclear correlations that exist in the true eigenstate.

This raises the important question regarding whether one has predictive power for other observables than the energy. The belief is that observables that can be calculated from the one-body densities that appear in the energy functionals should be trusted. In our case we calculate Coulomb and kinetic energies, which are given by densities that are included in the set of variational variables of the energy functional $\mathcal{E}[\mathbf{c}, \hat{\rho}]$ and therefore should be predicted with high accuracy.

In addition to these more general considerations there are also concerns about numerical precision. In the SkM* case the Coulomb energy difference $\Delta V_C = -0.307$ MeV $= (924.854 - 925.161)$ MeV is a result of subtracting two big numbers that have been calculated numerically. That means a precision of 10 keV for each of them is desirable. For SIII-HFB, where $\Delta V_C = 0.001$ MeV, a precision of 0.1 keV is needed. We have checked that we can reach enough numerical precision by sufficient iteration steps.

TABLE III. Violation of the Hellmann-Feynman theorem $\delta = \alpha_0[\partial E^{\text{tot}}(\alpha_0)/\partial\alpha] - E^{\text{Coul}}(\alpha_0)$ in HF and HFB calculations with SIII Skyrme functional for ^{228}Th.

HF	HFB (no cutoff)	HFB (with cutoff)
0.02 keV	0.5 keV	200 keV

But there is also the quest for accuracy. Let us, for example, consider the approximate treatment of the exchange term. Its contribution in HFB-SIII is -34 MeV, a 10% error means already 3 MeV uncertainty in $\langle V_C \rangle = V_C^{\text{direct}} + V_C^{\text{exch}}$. However, one would expect that this is mainly a systematic error that is similar for the two states so that the difference should be less affected, but 1% still means 0.3 MeV error. The actual situation for SIII-HFB is $\Delta V_C^{\text{direct}} = 0.29$ keV and $\Delta V_C^{\text{exch}} = 0.71$ keV that adds up to the $\Delta V_C = 0.001$ MeV listed in Table I. In this case the approximate exchange term gives the larger contribution that weakens strongly the confidence in the calculated value of the sensitivity.

As discussed in Sec. II the proper derivation of the equations of motion from an energy functional is crucial for the validity of the Hellmann-Feynman theorem. Without this theorem one would calculate numerically the derivative of the energy with respect to α and create a new source of numerical errors. We tested the validity of the Hellmann-Feynman theorem by comparing to numerical derivatives using a five-point formula. In Table III the deviations are listed for the ^{228}Th ground state of the SIII functional. In the HF calculation the deviation is within the numerical uncertainty induced by the five-point formula. In the HFB calculation one gets also sufficient accuracy when no cutoff in the quasiparticle subspace contributing to the pairing interaction is applied. But the accuracy drops by three orders of magnitude when the density matrices and pairing tensors are calculated by including contributions from quasiparticle states up to the cutoff energy of 60 MeV. The reason is that this truncation violates the variational structure of the HFB equations [57]. For most observables, this violation induces small effects, and usually can be safely neglected, but it does show up in the very demanding calculation of the Coulomb energy differences.

As discussed before, another accuracy issue is the fact that our model does not contain projection on good total spin and sharp particle number. Also the possibility that configurations could admix that consist of the $K^\pi = 1^-$ band of ^{228}Th coupled with a single-neutron $5/2^-$ state cannot be excluded. These questions have to be the task of future investigations.

VI. SUMMARY

We have investigated the lowest two states of ^{229}Th that are almost degenerate in energy. Two very successful energy functionals SkM* and SIII have been employed in a density-matrix functional theory. Hartree-Fock and Hartree-Fock-Bogoliubov calculations have been performed and compared. The result is that for the SkM* functional the difference in Coulomb energy ΔV_C between excited and ground state ranges from 450 keV without pairing to -300 keV when pairing effects are included. However, the SIII-HFB result gives $\Delta V_C = 1$ keV only. The differences in neutron and proton kinetic energies are of similar size and also quite different for SkM* and SIII.

Altogether, the nuclear models we used predict sensitivities, $q_s = \Delta V_C/h$, of the drift of the transition frequency $\delta\nu/\nu$ on relative changes $\delta\alpha/\alpha$ in the fine structure constant, that have absolute values varying between about 400 keV or 10^{20} Hz and 1 keV or 2×10^{17} Hz. We have pointed out and discussed the fact that the pairing correlations smooth out polarization effects exerted by the single-particle orbitals. Therefore, such correlations not only dramatically decrease the anticipated sensitivity but also make their determination very uncertain, due to dependence on very detailed properties of the mean-field and pairing effects.

We have also performed spherical calculations and conclude that spherical models should not be consulted as they are too far from reality to provide serious numbers.

As even the sign of the sensitivity is uncertain, much more refined calculations are needed that include coupling to low-lying core excitations and projection on eigenstates with good total angular momentum and particle number. Before being able to provide reasonably trustable numbers how the transition energy varies as function of the fine structure constant α one has to make sure that the model reproduces the three low-lying rotational $K^\pi = 5/2^+, 3/2^+, 5/2^-$ bands up to $J \approx 9/2$ and the known electromagnetic transitions within the bands and between them. This would provide more confidence in the quality of the many-body states and their Coulomb energy.

In any case the calculations must treat all nucleons (no inert core) because the whole effect comes from a subtle polarization of the core protons. Furthermore, the model has to be of variational type to make use of the Hellmann-Feynman theorem. Without that one cannot be sure that the polarization effects caused by the strong interaction are treated consistently with the necessary accuracy. Rough estimates and simple minded models are not sufficient.

The experimental endeavor for measuring the drift of the transition frequency in ^{229}Th has to be accompanied by substantially improved models on the nuclear theory side and attempts to gain experimental information on the Coulomb energies via radii, quadrupole moments, or even form factors. Without a concerted action of experimental and theoretical efforts the goal of improved limits on the temporal drift of fundamental constants cannot be reached.

ACKNOWLEDGMENTS

E.L. acknowledges fruitful discussions with E. E. Kolomeitsev and D. N. Voskresensky. This work was supported in part by the Polish Ministry of Science under Contract No. N N202 328234 and by the Academy of Finland and University of Jyväskylä within the FIDIPRO programme. V.V.F. acknowledges support from Australian Research Council and Marsden grant.

[1] T. Rosenband, D. B. Hume, P. O. Schmidt, C. W. Chou, A. Brusch, L. Lorini, W. H. Oskay, R. E. Drullinger, T. M. Fortier, J. E. Stalnaker *et al.*, Science **319**, 1808 (2008).
[2] T. M. Fortier, N. Ashby, J. C. Bergquist, M. J. Delaney, S. A. Diddams, T. P. Heavner, L. Hollberg, W. M. Itano, S. R. Jefferts, K. Kim, F. Levi, L. Lorini, W. H. Oskay, T. E. Parker, J. Shirley, and J. E. Stalnaker, Phys. Rev. Lett. **98**, 070801 (2008).
[3] E. Peik, B. Lipphardt, H. Schnatz, T. Schneider, C. Tamm, and S. G. Karshenboim, Phys. Rev. Lett. **93**, 170801 (2004).
[4] M. Fischer, N. Kolachevsky, M. Zimmermann, R. Holzwarth, T. Udem, T. W. Hänsch, M. Abgrall, J. Grünet, I. Maksimovic, S. Bize *et al.*, Phys. Rev. Lett. **92**, 230802 (2004).
[5] J. D. Prestage, R. L. Tjoelker, and L. Maleki, Phys. Rev. Lett. **74**, 3511 (1995).
[6] V. V. Flambaum, Eur. Phys. J. Special Topics **163**, 159 (2008).
[7] S. N. Lea, Rep. Prog. Phys. **70**, 1473 (2007).
[8] S. N. Lea, Eur. Phys. J. Special Topics **163**, 37 (2008).
[9] A. C. Hayes and J. L. Friar, Phys. Lett. **B650**, 229 (2007).
[10] E. Peik and C. Tamm, Europhys. Lett. **61**, 181 (2003).
[11] V. V. Flambaum, Phys. Rev. Lett. **97**, 092502 (2006).
[12] B. R. Beck, J. A. Becker, P. Beiersdorfer, G. V. Brown, K. J. Moody, J. B. Wilhelmy, F. S. Porter, C. A. Kilbourne, and R. L. Kelley, Phys. Rev. Lett. **98**, 142501 (2007).
[13] E. V. Tkalya, A. N. Zherikhin, and V. I. Zhodov, Phys. Rev. C **61**, 064308 (2000).
[14] A. M. Dykhne and E. V. Tkalya, J. Exp. Theor. Phys. Lett. **67**, 251 (1998).
[15] V. A. Dzuba, V. V. Flambaum, and J. K. Webb, Phys. Rev. Lett. **82**, 888 (1999).
[16] V. A. Dzuba, V. V. Flambaum, and J. K. Webb, Phys. Rev. A **59**, 230 (1999).
[17] V. A. Dzuba and V. V. Flambaum, Phys. Rev. A **61**, 034502 (2000).
[18] V. A. Dzuba and V. V. Flambaum, Phys. Rev. A **77**, 012515 (2008).
[19] A. T. Nguyen, D. Budker, S. K. Lamoreaux, and J. R. Torgerson, Phys. Rev. A **69**, 022105 (2004).
[20] H. Hellmann, Z. Physik **85**, 180 (1933).
[21] R. P. Feynman, Phys. Rev. **56**, 340 (1933).
[22] J. Goodisman, Phys. Rev. A **2**, 1 (1970).
[23] R. Roth, P. Papakonstantinou, N. Paar, H. Hergert, T. Neff, and F. H., Phys. Rev. C **73**, 044312 (2006).
[24] R. Roth, T. Neff, H. Hergert, and H. Feldmeier, Nucl. Phys. **A745**, 3 (2004).
[25] T. Neff and H. Feldmeier, Nucl. Phys. **A713**, 311 (2003).
[26] J. Boguta and A. R. Bodmer, Nucl. Phys. **A292**, 413 (1977).
[27] J. D. Walecka, Ann. Phys. (NY) **83**, 491 (1974).
[28] W. Kohn and L. J. Sham, Phys. Rev. **140**, A1133 (1965).
[29] Y. M. Engel, D. M. Brink, K. Goeke, S. J. Krieger, and D. Vautherin, Nucl. Phys. **A249**, 215 (1975).
[30] P. Ring, Prog. Part. Nucl. Phys. **37**, 193 (1996).
[31] M. Bender, P.-H. Heenen, and P.-G. Reinhard, Rev. Mod. Phys. **75**, 121 (2003).
[32] P. Ring and P. Schuck, *The Nuclear Many-Body Problem* (Springer-Verlag, New York, 1980).
[33] J. Dobaczewski, W. Nazarewicz, T. R. Werner, J. F. Berger, C. R. Chinn, and J. Dechargé, Phys. Rev. C **53**, 2809 (1996).
[34] S. Krewald, V. B. Soubbotin, V. I. Tselyaev, and X. Viñas, Phys. Rev. C **74**, 064310 (2006).
[35] U.-G. Meißner, A. M. Rakhimov, A. Wirzba, and U. T. Yakhshiev, Eur. Phys. J. A **31**, 357 (2007).
[36] V. V. Flambaum and E. V. Shuryak, Phys. Rev. D **65**, 103503 (2002).
[37] V. V. Flambaum and E. V. Shuryak, Phys. Rev. D **67**, 083507 (2003).
[38] V. V. Flambaum, A. Höll, P. Jaikumar, C. D. Roberts, and S. V. Wright, Few-Body Systems **38**, 31 (2006).
[39] V. V. Flambaum, D. B. Leinweber, A. W. Thomas, and R. D. Young, Phys. Rev. D **69**, 115006 (2004).
[40] G. Audi, A. H. Wapstra, and C. Thibault, Nucl. Phys. **A729**, 3 (2003).
[41] Y. K. Gambhir, P. Ring, and A. Thimet, Ann. Phys. (NY) **198**, 132 (1990).
[42] J. Dobaczewski and P. Olbratowski, Comput. Phys. Commun. **158**, 158 (2004); J. Dobaczewski, J. Dudek, and P. Olbratowski, nucl-th/0501008.
[43] J. Dobaczewski, W. Satuła, J. Engel, P. Olbratowski, P. Powałowski, M. Sadziak, A. Staszczak, M. Zalewski, and H. Zduczuk, Comput. Phys. Commun. (to be published); arXiv:0903.1020v1.
[44] M. Beiner, H. Flocard, N. Van Giai, and P. Quentin, Nucl. Phys. **A238**, 29 (1975).
[45] J. Bartel, P. Quentin, M. Brack, C. Guet, and H.-B. Håkansson, Nucl. Phys. **A386**, 79 (1982).
[46] M. Zalewski, J. Dobaczewski, W. Satuła, and T. R. Werner, Phys. Rev. C **77**, 024316 (2008).
[47] A. Bohr and B. R. Mottelson, *Nuclear Structure* (World Scientific, Singapore, 1998).
[48] G. A. Lalazissis, J. König, and P. Ring, Phys. Rev. C **55**, 540 (1997).
[49] Xiao-tao He and Zhong-zhou Ren, Nucl. Phys. **A806**, 117 (2008).
[50] A. C. Hayes, J. L. Friar, and P. Möller, Phys. Rev. C **78**, 024311 (2008).
[51] E. Ruchowska, W. A. Płóciennik, J. Żylicz, H. Mach, J. Kvasil, A. Algora, N. Amzal, T. Bäck, M. G. Borge, R. Boutami *et al.*, Phys. Rev. C **73**, 044326 (2006).
[52] V. Barci, G. Ardisson, G. Barci-Funel, B. Weiss, O. El Samad, and R. K. Sheline, Phys. Rev. C **68**, 034329 (2003).
[53] D. G. Burke, P. E. Garrett, T. Qu, and R. A. Nauman, Nucl. Phys. **A809**, 129 (2008).
[54] K. Gulda, W. Kurcewicz, A. J. Aas, M. J. G. Borge, D. G. Burke, B. Fogelberg, I. S. Grant, E. Hagebø, N. Kaffrell, J. Kvasil *et al.*, Nucl. Phys. **A703**, 45 (2002).
[55] V. G. Soloviev, *Theory of Complex Nuclei* (Pergamon, Oxford, 1976).
[56] E. Litvinova and P. Ring, Phys. Rev. C **73**, 044328 (2006).
[57] J. Dobaczewski, P. Borycki, W. Nazarewicz, and M. V. Stoitsov (to be published).